Check for updates

Critical review on the chemical reduction of nitroaniline

Muhammad Imran Din, [ID] *[a] Rida Khalid,[a] Zaib Hussain,[a] Jawayria Najeeb, [ID] [b] Ahsan Sahrif,[a] Azeem Intisar [ID] [a] and Ejaz Ahmed[a]

Conversion of nitroaniline (NA), a highly toxic pollutant that has been released into aquatic systems due to unmanaged industrial development in recent years, into the less harmful or a useful counterpart is the need of the hour. Various methods for its conversion and removal have been explored. Owing to its nominal features of advanced effectiveness, the chemical reduction of 4-NA using various different nanocatalytic systems is one such approach that has attracted tremendous interest over the past few years. The academic literature has been confined to case studies involving silver (Ag) and gold (Au) nanoparticles, as these are the two most widely used materials for the synthesis of nanocatalytic assemblies. Focus has also been given to sodium borohydride ($NaBH_4$), which is used as a reductant during the chemical reduction of NA. This systematic review summarizes the fundamentals associated with the catalytic degradation of 4-NA, and presents a comprehensive and critical study of the latest modifications used in the synthesis of these catalytic systems. In addition, the kinetics, mechanisms, thermodynamics, as well as the future directions required for understanding this model reaction, have been provided in this particular study.

Introduction

Among various industrial pollutants, particularly nitro-aromatic compounds, removal methodologies associated with 4-nitroaniline (4-NA) have attracted much attention due to its hazardous and deleterious effects.[1] 4-NA is a non-biodegradable, chemically resistive, highly reactive noxious waste and a persistent pollutant.[2] In addition, 4-NA is excessively utilized in different industries as a raw material, including the synthesis of dyes, pharmaceutical products, gum inhibitors, antioxidants, poultry medicines, corrosion inhibitor, explosives, and pesticides. Owing to these particular uses, 4-NA is regularly released into aquatic reservoirs as the main component of the poorly treated industrial effluent. Consequently, 4-NA directly affects aquatic life and indirectly influences human beings as well. Since 4-NA is a colored pollutant, its presence in the aquatic system hinders the entry/penetration of sunlight into the oceans, causing a decrease in the rate of photosynthesis. Ultimately, this not only adversely affects the plants, but also the aquatic fauna consuming those plants. Moreover, the presence of the nitro group in the compound is highly dangerous, as it possesses strong electron-withdrawing tendencies and can lead to the formation of explosives in the aqueous environment.[3] Owing to

its hazardous nature and adverse effects, the National Environmental Protection Agency (NEPA) of the People's Republic of China enlisted 4-NA as a priority hazardous pollutant for aquatic life.[4,5] In terms of its direct inhalation and ingestion, the long term exposure to 4-NA can induce many health problems in humans, including dyspnea, irritability, vomiting, diarrhea, convulsions, respiratory arrest, anemia, and jaundice.[6] Keeping these concerns in mind, the elimination or removal of 4-NA from the aqueous reservoirs is a highly significant process. A flood of academic reports can be found in the scientific literature in recent years, where the effort has been made to present solutions to this particular problem.[7]

Numerous methodologies (such as adsorption, membrane filtration, flocculation, biological, advanced oxidation processes, hydrothermal, and catalytic reduction) have been utilized for the treatment of nitroaromatic pollutants.[8-13] The adsorption removal process possesses certain advantages, including low cost (raw material for the adsorbent is cheap), green synthesis and absence of the by-products, but certain limitations have been observed with the application of this process. Disadvantages such as multistep preparatory routes, incomplete removal efficacy, expensive recovery processes and the requirement of additional setups (for the separation of the adsorbate from the adsorbent) make this process undesirable.[9,14-19] Membrane filtration processes suffer from the drawbacks of complicated preparation procedures, high maintenance costs, incomplete removal of the pollutant and fouling/breakage of the membranes. Problems such as the formation of huge amounts of sludge, sludge disposal and high cultivation costs for bioflocculants limit the use of the

[a] Institute of Chemistry, University of the Punjab, New Campus, Lahore 54590, Pakistan. E-mail: imrandin2007@gmail.com; ridakhalid42@gmail.com; chahsansharif@yahoo.com; azeemchemist@yahoo.com; dr.ijaz.ahmad@gmail.com; drzh1972@hotmail.com; Fax: +92-42-99231269; Tel: +92-33-19743520

[b] Department of Chemistry, University of Gujrat, Gujarat 50700, Pakistan. E-mail: jiyanajeeb73@gmail.com

bioflocculation methodology.[20,21] Although the use of biological species to carry out biodegradation has also been exploited, low conversion/degradation rates and high time consumption makes it a less effective methodology for removal.[8,22] Methodologies based on the chemical approach are divided into two categories. The photocatalysis-based advanced oxidation treatment is highly effective in terms of degradation, but the difficulties in manipulating the reaction parameters (due to the involvement of free radicals), and its high cost for the preparation and maintenance of the irradiation setups are still some serious issues that need to be addressed for the effective use of this approach.[23–28] Nanomaterial-based chemically induced catalytic reduction is another removal approach that has enjoyed a tremendous spotlight in recent years because of its numerous advantages, including its effective and fast conversion rates, economical preparatory routes and the absence of sludge. The deleterious effects of 4-NA are dealt by converting the nitro group of the pollutant into an aniline group. This acquired 4-phenylenediamine (4-PDA) product is further utilized as a precursor/rawmaterial in various industries (for instance, during the preparation of various surfactants, polymers, rubber, antioxidants, photograph developer and dyes).[3] Therefore, the catalytic conversion of 4-NA into 4-PDA is an industrially useful process that has been extensively exploited in academic research for the past ten years. It is an exemplary reaction for investigating the catalytic potential of the newly engineered nanocatalytic systems owing to its significance and relative ease.[29–32]

This review attempted to organize the particular case studies involving the catalytic conversion of 4-NA into its reduced counterpart and present an overall picture and fundamentals of this reaction for developing a better understanding of the new beginners hoping to exploit this important field of nanocatalysis. Most of the reviews written in this field are generalized (*i.e.*, involves the whole class of the nitroaromatic pollutants[33–35]) and do not work on the specific model reaction. To the best of the author's information, no such review that completely focuses on 4-NA has been documented previously in the literature. Moreover, detailing recent advancements in the nanocatalytic systems used for the catalytic conversion of 4-NA will help in designing new synthetic approaches. Structurally, the review is composed of the following sections: introduction (encompassing a brief description of the problem), classification of the catalytic assemblies (according to the nature of the used stabilization medium), characterization techniques (used for studying the nanocatalytic systems and monitoring the progress of the catalytic reaction), fundamentals of the catalytic reaction (describing the basic physical chemistry of the 4-NA reaction) and summary/future directions. To summarize the literature and facilitate a better understanding of this topic, relevant data is also presented in tabulated form.

Classification of the nanocatalytic system

The chemical reduction of 4-NA is a thermodynamically favorable process. However, this reaction does not proceed in the absence of the catalyst owing to the presence of a large kinetic barrier between the reactants and products. Catalytic mediums essentially eliminate this problem by providing an electron-transferring surface for the interaction of the reactants. Nanomaterial-based catalytic assemblies further facilitate the reaction by providing a much larger surface area (owing to its small size in the nanometer range), in comparison to the conventional powdered catalysts (usually existing in the micrometer range) for the transfer of the electrons. Fundamentally, a single nanocatalytic system can be categorized into two parts. One portion is the nanomaterial, which is the basic electron-transducing surface responsible for the transfer of the electron from an electron-donating species (reductant) to the 4-NA molecule. Consequently, 4-NA is reduced by acquiring that released electron and is converted into 4-PDA. The supporting medium (which is responsible for keeping the nanomaterial in the nano-range by providing the immobilization surface for the nanomaterials) comprises the second portion of the nanocatalytic assemblies. Both portions are equally significant in determining the efficacy of the engineered nanocatalytic system.[35] In the present work, two types of classification are proposed that highlight both components of the nanocatalytic system. The classification that is based on the manufacturing route used for the preparation of the nanomaterials deals with the nano-range catalytic portion of the assembly, while the second classification that is based on the nature of the utilized stabilization medium highlights the significance of the support system in the nanocatalytic assembly.

Route of manufacturing nanomaterials

The nanocatalytic assemblies can be mostly divided into two categories. The case studies regarding these categories are summarized in Table 1.

Chemical synthesis

The chemical synthesis of metal NPs involves different chemical reagents, particularly reducing agents (such as sodium borohydride, potassium borohydride, hydrazine, and hydrogen gas), for the reduction of metallic ions acquired from the metal precursor salt. The reduction of metallic ions leads to the formation of metallic atoms, and a number of metallic atoms in their zero-valent state aggregate to form metal NPs. Zhou *et al.*[36] documented the synthesis of silver nanoparticles (Ag NPs) using a chemical route that involved the flashing of a hot saturated solution of silver oxide (Ag_2O) in the presence of hydrogen gas. A color change (*i.e.*, from the colorless medium to the appearance of a green color) indicated the formation of the Ag NPs. Another study documents the preparation of the Ag NPs stabilized on a porous silicon (Psi) based glass slide by treating a mixture of silver nitrate ($AgNO_3$) with hydrogen fluoride (HF) in the presence of the dipped Psi slide. The engineered NPs were deposited on the slide and removed afterward by putting the slide in a nitric acid solution.[37] Vadakkekara *et al.*[38] prepared Ag NPs in the presence of gelatin using solutions of $AgNO_3$, sodium hydroxide (NaOH) and hydroxylammonium hydrosulphate. It

Table 1 Silver and gold catalysts prepared by utilizing different methodologies and supporting materials for 4-NA reduction

Supporting system	Catalyst system	MNPs	Methods	Reducing agent	Ref.
Green synthesis					
Soapnut shells	Au NPs	Au	Biosynthesized	Soapnut shells	50
Reduced graphene oxide	Ag NWs-rGO	Ag	Green synthesis, *i.e.*, seed-mediated or polyol one step method	—	52
Protein extract (*Pycnoporus sanguineus*)	Au NPs	Au	Biosynthesized	Protein extract (*Pycnoporus sanguineus*)	53
Leaf extract (*Elephantopus scaber*)	Ag NPs	Ag	Microwave assisted synthesis	Leaf extract (*Elephantopus scaber*)	54
Biosurfactant ethoxylated sterol	Au NPs BPS-30	Au	Tentative-growth mechanism	—	55
Chemical synthesis					
Cefditorene	Ag NPs	Ag	Chemical reduction	NaBH$_4$	42
Silica	Fe$_3$O$_4$/SiO$_2$/Ag	Ag	Sonochemical	NaBH$_4$	31
Glass slide	Immobilized Ag NPs	Ag	Self-assembly	NaBH$_4$	36
Porous silica (PSi)	Ag NPs/PSi chips	Ag	Not available	NaBH$_4$	37
Gelatin	Colloidal hollow silver nanoparticles	Ag	Chemical reduction method	NaBH$_4$	38
Quantum clusters (QCs)	Ag QCs	Ag	Interfacial etching method	NaBH$_4$	56
Polymer	PVP-Au NPs	Au	Microwave heating method	NaBH$_4$	57
Silica matrix	Ag NPs (SNSM)	Ag	Impregnation technique	NaBH$_4$	58
Microgels	Ag-P(NIPAM-AAc-AAm) hybrid microgels	Ag	Precipitation method	NaBH$_4$	59
Resorcinarene	RPAMA-capped Au NPs	Au	Not available	NaBH$_4$	60

was observed that the colloidal hollow Ag NPs were very stable and effective, having a size range of 10–40 nm. Kundu *et al.*[39] successfully prepared cetyltrimethylammonium bromide-terminated gold (Au) nanomaterials (including nanospheres, nanorods, and nanoprisms). A seed-mediated approach was utilized for the preparation of the gold nanospheres and nanorods, while the microwave heating method was used for the gold nanoprisms. It was observed that the Au nanospheres proved to be an efficient catalyst, as compared to the nanorods and nanoprisms, owing to its smaller surface area. Additionally, bimetallic NPs have gained much attention due to their improved catalytic efficiency, as compared to monometallic assemblies. Bimetallic nanoparticles are composed of two different types of metal atoms coexisting in the segregated form in such a way that both atoms express their properties in conjugation with each other. Consequently, the catalytic efficacy of the bimetallic system is improved by the complementary nature of the two different nanoparticles.[40] Madavi *et al.*[41] synthesized a palladium (Pd)/nickel (Ni) bimetallic assembly by utilizing aerosol OT as a capping agent and hydrazine hydrate as the reductant. The engineered nanocatalyst was used for the reduction of 4-NA in an aqueous medium. It was observed that the lower concentration of the capping agent led to an ineffective immobilization of the NPs, which then led to the lowered degradation rates for 4-NA. Therefore, the concentration of the stabilizing agent and reductant must be optimized to acquire the best catalytic efficacies. Other crystallographic inorganic materials, such as bismuth sulfide (Bi$_2$S$_3$) crystals, can also be utilized as the nanomaterials.[42] Bi$_2$S$_3$ was found to be an efficient catalyst for the reduction of nitroaromatics.[43] The

preparation of Bi$_2$S$_3$ was performed by utilizing the wet chemical approach. However, further work must be done to ensure the stability of the NPs. It was observed that after successive usage, the shape of the nanocatalyst became altered, which led to a lower catalytic efficacy of the inorganic NPs.[44] Numerous other NPs, *e.g.*, copper (Cu),[45] platinum (Pt)[46] and (Pd),[47] were also synthesized using chemical approaches. These nanocatalytic assemblies were found to be a favorable candidate for the reduction of 4-NA.

Biological synthesis

Lately, many case studies reporting the use of biomaterials (such as extracts acquired from the leaves, stem, seeds of plants, algal culture and fungal culture) have been documented for the preparation of nanomaterials. This methodology is considered far superior in terms of its environment-friendly advantages than that of the chemical methodology. This green route uses certain aromatic compounds (*i.e.*, phenolics, flavonoids and other phytochemicals) naturally present in the biological extract for the dual purpose of stabilization and reduction. However, a clear difference in the immobilization capacities between the chemical and biological methods can be observed *via* micrographic techniques (*i.e.*, scanning electron microscopy (SEM) and transmission electron microscopy (TEM)). Almost all nanomaterials acquired from the biological methods show aggregation owing to less efficacy of the natural components to immobilize the nanoparticles.[48,49] Despite this drawback, the fact that this methodology does not utilize harmful and toxic chemicals for immobilization will always be considered the biggest benefit of using this approach. Reddy *et al.*[50]

successfully synthesized Au NPs from the *Sapindus mukorossi* Gaertn. fruit pericarp by varying the amount of the precursor chloroauric acid (HAuCl₄). It was observed that the NPs synthesized by using 1 mM of the precursor salt showed the best catalytic performance as compared to higher concentrations. Stability studies indicated that the Au NPs remained stable for 5 months. Dauthal et al.[51] reported the biosynthesis of Au NPs and Ag NPs using $HAuCl_4 \cdot 3H_2O$ and $AgNO_3$ solution with the agro-industrial waste of the *Citrus aurantifolia* peel extract. They observed that the peaks of the precursor salts disappeared in the UV-visible spectra, which showed that the biosynthesis of the Au NPs and Ag NPs started within 2 minutes of adding the extract into the medium. Biologically synthesized Au NPs using the extract of *Moringa oleifera* petals have also been documented for the reduction of 4-NA by Anand et al.[49] They reported that NaBH₄, which itself is a toxic compound but is utilized regularly as the reductant during the reduction process of 4-NA, is also converted into its metaborate form owing to this system, which is comparatively less toxic in nature in comparison to its general form. Shi et al.[48] synthesized Au NPs through a biological synthetic route using the intracellular protein extract of *Pycnoporus sanguineus*. The engineered Au NPs exhibited excellent potential for catalytic reduction. Regan and Banerjee[13] utilized a bimetallic catalyst for the reduction of 4-NA by synthesizing size-controlled Au–Pd bimetallic nanoparticles fabricated on porous *germania* nanospheres.

Supporting assemblies for development of nanomaterial

Based on the nature of the supporting media that can effectively stabilize the nanomaterials, the nanocatalytic assemblies can be divided into the following categories. Different organic materials (including ligands, surfactants, polymeric gels, and dendrimers) have been used abundantly as capping agents, as shown in Fig. 1. Organic materials are predominantly considered to be more advantageous in comparison to other stabilization media owing to their eco-friendlier and biodegradable characteristics. However, organic media are soft and flexible systems. The immobilization capacity of these media to fabricate the nano-material is a bit lower than that of rigid inorganic materials. Sometimes, the leaking of NPs from the medium has also been observed.[61] Recently, organic polymers of various types have gained a lot of attention for the immobilization of NPs.[45] Use of the polymers in the form of the surfactant and dendrimers has also been extensively exploited for the immobilization of the NPs. However, it is a rather outdated approach as the catalytic efficiency is reduced because of the presence of the outward coating of polymer around the NPs, which does not allow the pollutant to get attached to the NPs. Consequently, the catalytic efficiency is reduced. However, this drawback of the surfactants has been reduced by the preparation of advanced organic systems. One such advanced polymeric material is hydrogels/microgels, which consist of networks of polymeric chains interconnected to form the meshes of polymers that possess the ability to shrink/swell by the appropriate solvent.[62] The polymeric sieves act as a caging medium for the NPs and prevent the aggregation of NPs by keeping each NP trapped in a single sieve. The property of swelling and shrinkage in response to external stimuli (radiations, temperature and pH) is also helpful, as the process of the loading and fabrication of the NPs can be effectively carried out by this characteristic. The preparation of the NPs is facilitated by the swelled structure of microgels and once the NPs are formed, the system is de-swelled to provide a stabilizing coating of the
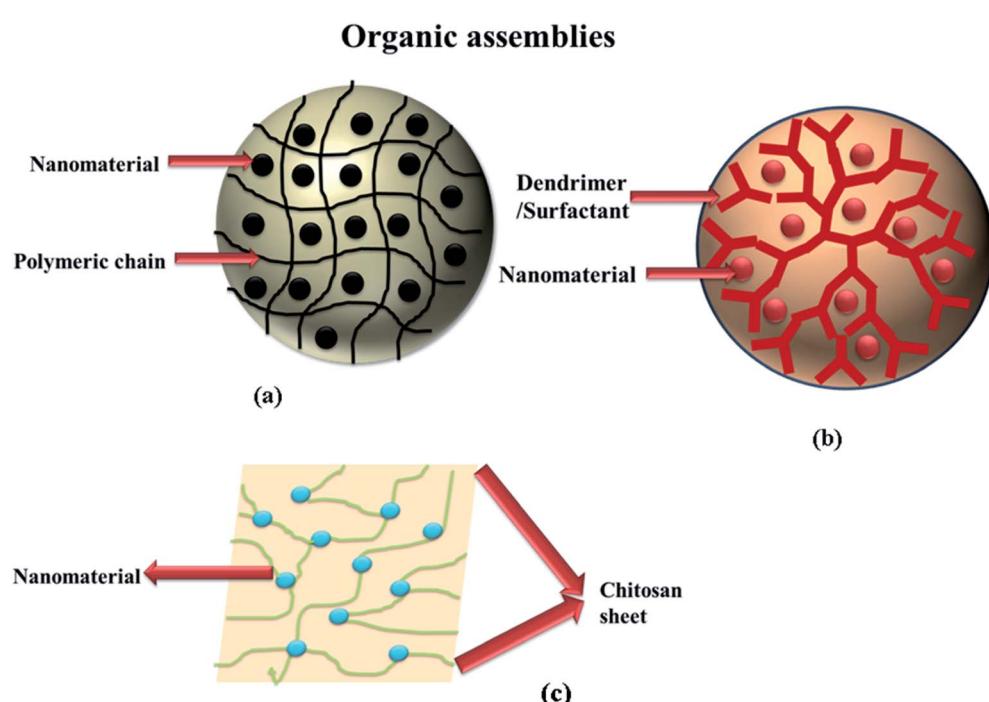

Fig. 1 Organic nanocatalytic assemblies: (a) polymeric gels/microgels, (b) dendrimer-stabilized system, (c) chitosan as a supporting material.

polymeric chains on the synthesized NPs.[6] Moreover, the preparative methodology for the synthesis and fabrication of hydrogels is also economical and inexpensive as compared to other materials. Free-radical precipitation polymerization is the most common route to synthesize the polymeric hydrogel medium, which is a single step method.[63] Additionally, these materials are nontoxic/biodegradable and do not suffer from any biodegradability drawbacks generally affiliated with the inorganic materials. Usually, the term "hybrid nanocatalytic assemblies" is coined for the hydrogels containing the immobilized NPs in its polymeric sieves, which is indicative of the fact that the resultant system can display the characteristics of both the polymers, as well as the nanoparticles.[64] Due to this particular reason, microgels are utilized in a variety of applications such as drug delivery, emulsion stabilization, immobilization of NPs, catalysis of harmful pollutants, preparation of photonic crystals, pH/temperature/ion sensors, surface coating material, diagnostics, and drug delivery applications.[65] Maity et al.[66] reported the synthesis of a sonication-induced hydrogel using asymmetric peptide-based bolaamphiphile molecules. The bolaamphiphile hydrogel was utilized for the fabrication of platinum (Pt) nanoparticles. Begum et al. manufactured poly(N-isopropylacrylamide) (p(Nipam))-based microgels for the stabilization of Ag NPs, which were then utilized for the reduction of 4-NA in the presence of reducing agents (NaBH$_4$).[59] Farooqi et al.[6] synthesized co-polymerized p(Nipam)-based microgels for the effective immobilization of Ag NPs to carry out the reduction of 4-NA to 4-PDA. They observed that the increase in the concentration of the nanocatalyst in the medium increased the catalytic efficacy of the reduction as the nanomaterial/surface area available for the 4-NA to get attached to the NPs increased alongside the concentration.

Other polymers such as poly(N-vinyl-2-pyrrolidone) (PVP)[57] and polyaniline (PANI)[47] are used as stabilizing agents for the immobilization of the NPs.[67] Scientists have also reported the presence of a host–guest relationship between the functional groups of the polymer molecules and the stabilizing substrate, which also facilitates the immobilization by providing a stress-free platform to the NPs.[47] Zhou et al.[36] designed a two-dimensional (2D) nanocatalytic assembly containing PVP-stabilized Ag NPs and utilized them for the reduction of 4-NA. They showed that the Ag NPs present on the 2D glass slide surface remained immobilized because of covalent and electrostatic attractions between the PVP and glass substrates. Tumma and Srivastava[47] deposited copper nanoparticles (Cu NPs) inside meso-PANI. The comparative study between the incorporation of Cu NPs and the copper (Cu(I) and Cu(II)) salts inside the PANI mesopores revealed that meso-PANI-containing Cu NPs were more efficient nanocatalysts than the copper salts. The authors also observed that the porous structure of the polymer was not only helpful in the immobilization (by providing the necessary space for the NPs to interact with the polymer), but also facilitated the catalytic process by removing the diffusional barrier faced by the reactant (pollutant) to reach the Cu NP surface. Similar results were reported by Liang et al.[68] in terms of the increase in the catalytic efficacy owing to the porous nature of the polymeric material. They utilized aminolyzed poly-oxymethylene/poly(L-lactide) (POM/PLLA) nanofibrous membranes (NFMs) for the immobilization of Ag NPs, and reported that the POM/PLLA-Ag NFMs catalyst showed superior catalytic performance for the reduction of 4-NA owing to the availability of increased active surface areas and the porous nature of POM/PLLA.
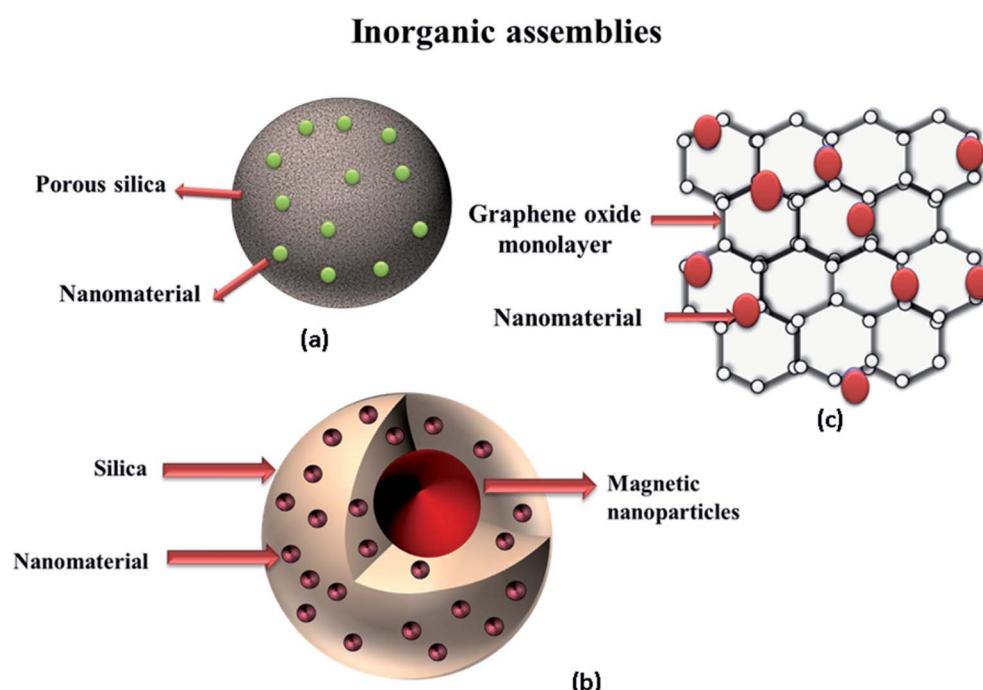

Fig. 2 Inorganic supporting nanocatalytic assemblies: (a) metal nanoparticles impregnated on porous silica, (b) nanomaterial-decorated silica-coated magnetic nanoparticles, (c) graphene oxide sheet containing nanomaterial.

Table 2 Organic and inorganic assemblies used for the catalytic reduction of 4-NA

Assemblies	Nanocatalytic assembly						Catalytic reduction of 4-NA			
	Nano-material	Fabrication medium	Reductant/oxidant	Diameter (nm)	Pollutant	Recyclability	Reductant	Solvent	Reaction settings	Ref.
Organic	Ag	Polyoxymethylene/poly(L-lactide) (POM/PLLA) nanofibrous membranes (NFMs)	1,6-Hexanediamine/2 propanol	7.6 ± 2.5	4-NA	4	$NaBH_4$	Aqueous solution	[Catalyst] = —; [4-NA] = 0.15 × 10^{-3} M; [NaBH$_4$] = 15 × 10^{-3} M	72
Organic	Os	DNA	Ethanol	1.5 ± 0.2	4-NA, 2-NA, 4-NP, 2-NP and MB	—	$NaBH_4$	Aqueous solution	[Catalyst] = 10 μL, [4-NA] = 1 × 10^{-3} M, [NaBH$_4$] = 1 × 10^{-1} M	73
Organic	Pt	Peptide bolaamphiphiles	Phosphate buffer	1–3	4-NA	—	$NaBH_4$	Aqueous solution	[Catalyst] = 1 × 10^{-2} M, [4-NA] = 5 mg, [NaBH$_4$] = 6 mg	66
Organic	Ni	Starch	Fe_3O_4	20–50	4-NA, 2-NA, 3-NA, 2-NT, 3-NT, 4-NT, 2-NP, 3-NP, 4-NP, 2-NBA, 3-NBA, 4-NBA, and other nitroaromatics	3	$NaBH_4$	Aqueous solution	[Catalyst] = 12 mg, [4-NA] = 3.62 ×10^{-2} M [NaBH$_4$] = 1.44 × 10^{-3} M	74
Organic	Ag	Polyurethane/keratin nanofibrous mats	Hexafluoro-2-isopropanol (HFIP) and electro-spinning	70	4-NA	5	$NaBH_4$	Aqueous solution	[Catalyst] = 0.025 g mL^{-1}, [4-NA] = 1 × 10^{-3} M, [NaBH$_4$] = 5 × 10^{-2} M	75
Inorganic	MnO	Iron oxide Fe_3O_4	Perilla frutescens leaf extract solution	0.67	4-NA, RhB	5	$NaBH_4$	Aqueous solution	[Catalyst] = 2 mg mL^{-1}, [4-NA] = 25 × 10^{-6} M, [NaBH$_4$] = 2 × 10^{-1} M	76
Organic	Pt-Ni	Cetyl trimethyl ammonium bromide (CTAB) micelle	N_2H_4	19 ± 3	4-NP, 2-NP, 4-NA, 4-AP	—	$NaBH_4$	Aqueous solution	[Catalyst] = 4.0 μg, [4-NA] = 8.5 × 10^{-5} M, [NaBH$_4$] = 1.2 × 10^{-2} M	77
Inorganic	CuNi	Co_3O_4	Cetyl trimethyl ammonium bromide (CTAB) and NaBH$_4$	19 ± 3	4-NP, 4-NA, 3-NA, 4-NT, 2-NA	6	$NaBH_4$	Aqueous solution	[Catalyst] = 2.0 mg, [4-NA] = 2 × 10^{-3} M L^{-1}, [NaBH$_4$] = 2 × 10^{-2} M L^{-1}	78
Inorganic	Ag	Fe_3O_4 nanocubes, silica	Ultrasonication, high temperature and pressure	10–20	4-NA	15	$NaBH_4$	Aqueous solution	[Catalyst] = 1 × 10^{-3} M, [4-NA] = 1 × 10^{-3} M, [NaBH$_4$] = 1 × 10^{-2} M L^{-1}	31
Organic	Au	Amphiphilic pillararene	Ascorbic acid	6.5 ± 1.4	4-NA	20	$NaBH_4$	Aqueous solution	[Catalyst] = —, [4-NA] = 1 × 10^{-4} M L^{-1}, [NaBH$_4$] = 8 × 10^{-3} M	79

Table 2 (Contd.)

| Assemblies | Nanocatalytic assembly | | | | | Catalytic reduction of 4-NA | | | |
	Nano-material	Fabrication medium	Reductant/oxidant	Diameter (nm)	Pollutant	Recyclability	Reductant	Solvent	Reaction settings	Ref.
Organic	Au	Mesoporous carbon	Ammonia solution	>5	2-NP, 4-NP, 2-NA, 4-NA	10	NaBH$_4$	Aqueous solution	[Catalyst] = 8.5 × 10^{-5} g, [4-NA] = 5 × 10^{-4} M, [NaBH$_4$] = 8 × 10^{-2} M	38
Inorganic	Ag	Silicon	Hydrofluoric acid	—	4-NA	—	NaBH$_4$	Aqueous solution	[Catalyst] = —, [4-NA] = 12 × 10^{-4} M, [NaBH$_4$] = 100 mg	37
Inorganic	Ag	Alumina	Quantum clusters and vacuum drying	—	4-NP, 4-NA	5	NaBH$_4$	Aqueous solution	[Catalyst] = 50 mg, [4-NA] = 7 × 10^{-3} M, [NaBH$_4$] = 160 × 10^{-3} M	56
Inorganic	Au	Graphene oxide	Microwave heating	50–350	4-NA	—	NaBH$_4$	Aqueous solution	[Catalyst] = 600 µL, [4-NA] = 1 × 10^{-3} M, [NaBH$_4$] = 1 × 10^{-1} M	71
Inorganic	Ag	Reduced graphene oxide	Abelmoschus esculentus vegetable	92	4-NA	—	NaBH$_4$	Aqueous solution	[Catalyst] = 10 µg, [4-NA] = 1 × 10^{-4} M, [NaBH$_4$] = 1 × 10^{-2} M	52
Organic	Cu, Ni, Co, Fe, Mn	Polyaniline	NaBH$_4$	4–10	4-NA	5	NaBH$_4$	Aqueous solution	[Catalyst] = 1 × 10^{-5} M, [4-NA] = 1 × 10^{-3} M, [NaBH$_4$] = 5 × 10^{-3} M	47
Organic	Au	Poly(N-vinyl-2-pyrrolidone) (PVP)	Microwave heating	22 ± 1.2	4-NA	—	NaBH$_4$	Aqueous solution	[Catalyst] = —, [4-NA] = 1 × 10^{-3} M, [NaBH$_4$] = 1 × 10^{-2} M	57
Organic	Au	1-Dodecyl-3-methylimidazolium bromide	Ascorbic acid, HNO$_3$	24.9 ± 3.6	4-NA, 4-NP	—	KBH$_4$	Aqueous solution	[Catalyst] = 300 µL, [4-NA] = 1 × 10^{-3} M, [KBH$_4$] = 1 × 10^{-1} M	30
Organic	Cu, Co, Ag	Chitosan	NaBH$_4$	5	4-NA, 4-NP, RhB	—	NaBH$_4$	Aqueous solution	[Catalyst] = 10 µL, [4-NA] = 1 × 10^{-3} M, [NaBH$_4$] = 1 × 10^{-2} M	69
Organic	Au-Pd	Reduced graphene oxide	Ultra-sonication and NaBH$_4$	5–15	4-NA	4	NaBH$_4$	Aqueous solution	[Catalyst] = 10 µL, [4-NA] = 1 × 10^{-3} M, [NaBH$_4$] = 1 × 10^{-2} M	80

Apart from the utilization of the synthetic polymers, biopolymers have also been utilized for the preparation of the nanocatalytic systems due to their favorable features, *e.g.*, acquisition from bio-renewable resources, biodegradability, nontoxic nature, and abundance of the source in nature. Bakhsh et al.[69] synthesized various cobalt (Co), Cu and Ag NPs supported on chitosan biopolymeric matrices, and used them as nanocatalysts for the degradation of 4-NA, 4-nitrophenol (4-NP) and rhodamine B (RhB). They observed that the natural presence of the amino and hydroxyl groups acted as the ligands for the successful synthesis of spherical shaped NPs having an average particle size of 5 nm. Gelatin is another biopolymer that has been widely used for the synthesis of drug carriers, hollow spheres and nanospheres due to its eco-friendly nature and cost-effectiveness. It has been reported to be used as a stabilizing and protective agent for the synthesis of Ag NPs.[38]

Rigid inorganic assemblies utilized for the immobilization of NPs are shown in Fig. 2. These inorganic assemblies show certain advantages over other stabilization materials. The materials can withstand severe operating conditions without losing their conformational properties. In addition, the rigidity of the inorganic material provides extraordinary stabilization to the NPs, and issues involving the leakage of the NPs are effectively avoided by utilizing these materials. However, these materials possess some shortcomings as well, including the requirement of lengthy/complicated preparative procedures and their non-biodegradable nature.

Silica is one of the widely used inorganic stabilization media owing to its properties, such as lesser density, high chemical resistivity, less toxicity, and high temperature resistivity. In comparison to other inorganic materials (alumina and graphene), the preparation and raw material acquisition are fairly easy. However, in terms of the manipulation of the morphological aspects, silica is a bit difficult to handle. This is the reason that most case studies involving silica require extremely high temperatures to acquire the ordered array of NPs stabilized by the silica molecules. Similar to the organic materials, the porous silica provides an additional advantage of increasing the surface area and reducing the diffusional barrier for the reactants to reach the NPs surface.[37] Liu et al.[37] reported the fabrication of Ag NPs on porous silicon (PSi). The presence of hydrogen fluoride (HF) led to the formation of Si–H bonds on the PSi surface, which facilitated the formation and immobilization of the Ag NPs. Ag NPs were easily dispersed owing to the porous nature of PSi, and the engineered nanocatalytic system showed excellent catalytic potential for the reduction of nitroaromatics. Ag NPs/PSi chips could also be easily separated from the reaction mixture by a simple centrifugation process. Graphene, a 2D single-layered carbon sheet exhibiting a honeycomb structure, is another inorganic material widely used for the incapacitation of the NPs.[52] Graphene sheets have quasi-planar sp[2] hybridized carbon atoms.[70] Its exceptional properties (including its remarkably high electrical, mechanical, thermal and optical properties) have been a surprise for researchers all around the world, which is the reason behind its extensive exploration in almost every walk of life.[71] Previously, the development of the single-walled graphene sheets was

considered a difficult task, but the improvements in the synthetic methodologies have now made it quite easy. Today, a huge number of case studies reporting the usage of graphene in nanotechnology-based applications can be found in the scientific literature.[70] Choi et al.[70] used graphene oxide (GO) nanosheets as the supporting medium for Au NPs, and found that the presence of the GO nanosheets exhibited synergic effects by enhancing the catalytic efficacy of the synthesized NPs. Apart from performing the function of the stabilization, GO also accelerated the catalytic reaction by conducting/shutting the electron itself as well. For acquiring defect-free graphene, the exfoliated procedures are widely used.[52] The chemical reduction method is another approach, where GO is converted into reduced graphene oxide (rGO). Because of the action of the reducing agents, such as hydrazine, dimethyl hydrazine or green reducing agents (including ascorbic acid, reducing sugar, amino acid, and green extracts), Gnanaprakasam and Selvaraju[52] used *Abelmoschus esculentus* (vegetable) extract for graphene reduction. Jasuja et al.[71] reported the synthesis of bare-surfaced Au NPs implanted on GO by utilizing the microwave treatment. Zhang et al.[46] reported the synthesis of 3D architectures, including hydrogels/aerogels, as the novel porous graphene-based material and used this assembly to fabricate the NPs. They prepared platinum (Pt) NPs stabilized on graphene aerogels (GA) (*i.e.*, Pt NPs/GA) through simple and efficient chemical methods. L-Cysteine was used as a reducing agent for the reduction of Pt ions into Pt NPs. During the preparation of GA, the graphene oxide was first converted into the hydrogels. The process of freeze-drying was then carried out afterward to convert the hydrogels into aerogels (the water present inside the polymeric sieves of the gels is replaced by air under a definite set of conditions). The engineered system has several advantages, such as the effective immobilization of the NPs by polymeric covering, the 3D open structure for the facile loading of the NPs, a highly efficient catalytic system owing to the synergistic electron-shuttling effects of the electrons *via* graphene, and the absence of diffusional barriers to the dye molecules owing to the open structure of the aerogels. The
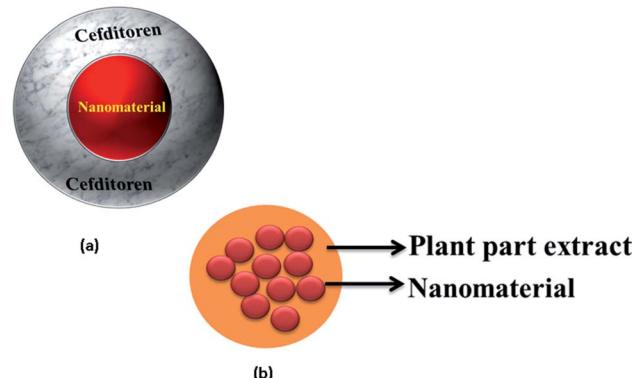

Fig. 3 Biogenic nanocatalytic assemblies: (a) cefditoren as an antibiotic, (b) nanomaterial stabilized by plant parts.
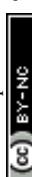
Table 3 Biogenic assemblies for the catalytic degradation of 4-NA

Nanocatalytic assembly						Catalytic reduction of 4-NA			
Nanomaterial	Fabrication medium	Plant part	Diameter (nm)	Pollutant	Recyclability	Reductant	Solvent	Reaction settings	Ref.
Ag	Tamarindus indica	Seed	40	2-NA, 4-NA	—	NaBH$_4$	Aqueous solution	[Catalyst] = 5×10^{-1} mL, [4-NA] = 1×10^{-3} M, [NaBH$_4$] = 5×10^{-2} M	81
Au	Citrus aurantifolia	Fruit	6 ± 46	4-NA	—	NaBH$_4$	Aqueous solution	[Catalyst] = 1×10^{-1} mg mL^{-1}, [4-NA] = 2×10^{-3} M L^{-1}, [NaBH$_4$] = 2×10^{-2} M L^{-1}	51
Au	Sapindus mukorossi Gaertn.	Fruit	9	4-NA	6 cycle	NaBH$_4$	Aqueous solution	[Catalyst] = 1×10^{-3} M, [4-NA] = 1×10^{-3} M, [NaBH$_4$] = 1×10^{-2} M	50
Au	Moringa oleifera	Flower	3–5	4-NP, 4-NA	—	NaBH$_4$	Aqueous solution	[Catalyst] = —, [4-NA] = 2×10^{-4} M, [NaBH$_4$] = 15×10^{-2} M	49
Au	Pycnoporus sanguineus	Protein	61.47–29.30	4-NA	—	NaBH$_4$	Aqueous solution	[Catalyst] = 0.19 mg mL^{-1}, [4-NA] = 5×10^{-4} M, [NaBH$_4$] = 5×10^{-2} M	48
Ag	Cnidium officinale	Rhizome	9	4-NA	—	NaBH$_4$	Aqueous solution	[Catalyst] = 0.02 mL, [4-NA] = 1×10^{-2} M, [NaBH$_4$] = 5×10^{-2} M	82
Ag	Cefditorene	—	14.1 ± 2.2	2-NA, 3-NA, 4-NA	—	NaBH$_4$	Aqueous solution	[Catalyst] = —, [4-NA] = 4×10^{-4} M, [NaBH$_4$] = 1×10^{-2} M	42
Au–Pd	Porous germania nanospheres	Fruit	7–10	4-NA	—	HCOONa	Aqueous solution	[Catalyst] = 0.1 mg, [4-NA] = 3 mg mL^{-1}, [HCOONa] = 1×10^{-2} M	13

synthesized system exhibited copacetic potential for carrying out the catalytic reaction in the case of 4-NA. Specific studies associated with these organic and inorganic supporting systems are summarized in Table 2.

Biogenic assemblies utilize numerous chemical compounds, which are naturally present inside the biomass, as a means to reduce and stabilize the engineered NPs. These natural compounds (including polyphenols, flavonoids, carotenes, xanthophyll, and other aromatic compounds) are isolated from the biomass in the form of the extracts, which are subsequently employed for the formation of the nanocatalytic assemblies. Fig. 3 illustrates the biogenic assemblies utilizing the natural compounds as the supports for the development of the nano-materials. Anand et al.[49] engineered Au NPs by using the petal extract of Moringa oleifera. The extract was utilized as the reducing and capping agent. Au NPs showed better and enhanced catalytic performance for the reduction of 4-NA. Dauthal et al.[51] synthesized Au NPs and Ag NPs using the agro-industrial waste of the Citrus aurantifolia peel extract, and utilized it as a catalyst for the reduction of 4-NA. The catalyst showed excellent performance for the degradation of 4-NA, as previously reported in many studies, but an aggregation of the nanomaterial was observed in some localized areas. This is one of the drawbacks of using this supporting medium, as it still lacks the effective immobilization capacities in comparison to other supporting media. Therefore, more studies and further research are required to address this problem of short-term stability in the case of biogenic assemblies. Recently, another approach has also been exploited where the antibiotics containing modified natural compounds were utilized as the stabilization medium for the fabrication of the nanoparticles. Cefditorene is a third generation oral antibiotic, and can be used as a stabilizing and protective agent for the incapacitation of the NPs. Junejo et al.[42] utilized cefditorene as a support for the synthesis of Ag NPs. It was observed that cefditorene-derived Ag NPs showed good catalytic conversion of 4-NA into 4-PDA. Yao et al.[60] utilized resorcinarene, a cyclic oligomer, as a support for Au NPs. Specific studies associated with these biogenic supporting assemblies are summarized in Table 3.

Organic–inorganic composite materials, possessing the combined characteristics of both organic and inorganic materials accumulated in a single system, are currently considered the most advanced and innovative form of supporting material for the immobilization of NPs. Not long ago, the designing of the hybrid supporting media was generally suggested under the future perspective for the particular reviews written in the field of the reduction of nitroaromatics.[3,61] Given the advancements in the field of material engineering, several case studies reporting such systems can be found in the academic literature these days. Fig. 4 pictorially depicts an organic–inorganic composite assembly used for the catalytic reduction of 4-NA. Generally, synthesis of the composite material involves the pre-modification of inorganic components by the organic material to develop well-organized and effective sites on the supporting medium for the efficient development of metal nanoparticles. Silica (SiO$_2$), an inorganic stabilizing material, is known for its high surface area (owing to its porous nature), but its

Organic-inorganic hybrid assemblies
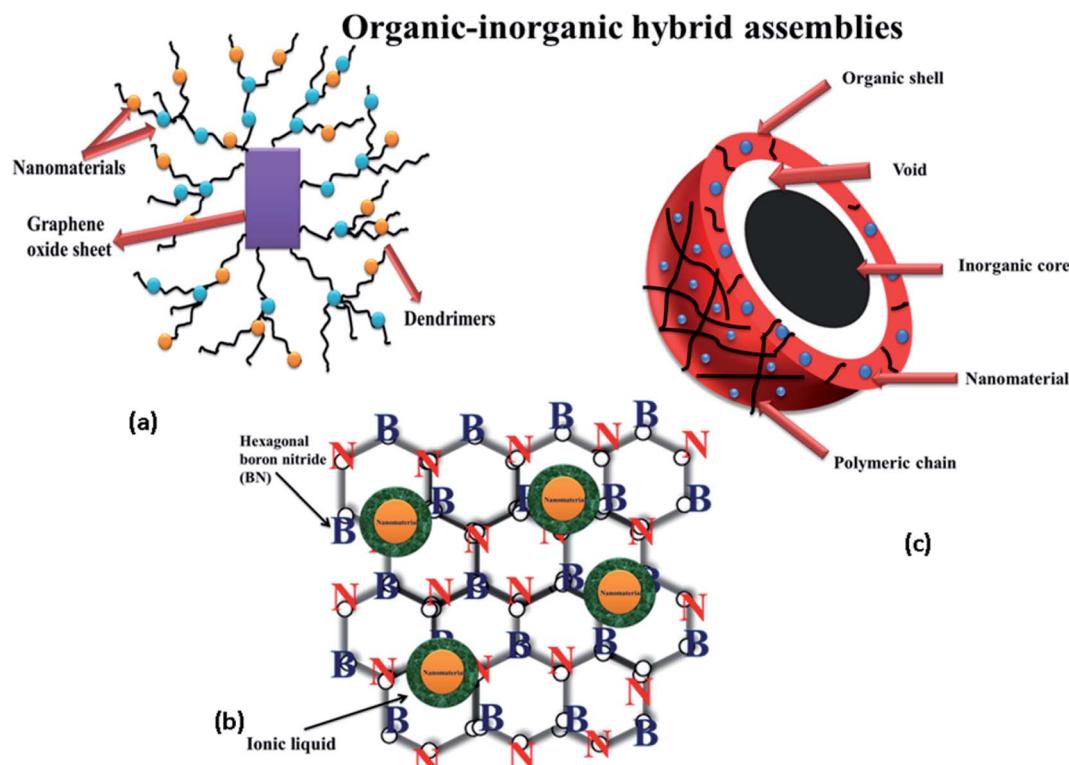
Fig. 4 Organic–inorganic composite nanocatalytic assemblies: (a) dendrimer and graphene supported nanomaterial, (b) hexagonal boron nitride containing nanomaterials and ionic liquid, (c) core–shell microgel.

processibility is rather difficult in its powdered form. Similarly, the organic material of chitosan exhibits phenomenal properties, but lacks mechanical strength. In addition, its degradability under extreme conditions limits its applicability as a stabilization medium. The drawbacks of both systems can be greatly countered by making a hybrid of the systems. Ali *et al.*[83] used inorganic–organic based assemblies (*i.e.*, chitosan-silica (CH-SiO$_2$) nanocomposite fiber) for the development of metal nanomaterials. They prepared various nanomaterials (including Cu, Co, Ag, and Ni assemblies) by using a combination of silica and chitosan (biopolymer), and observed that Cu/CH-SiO$_2$ showed the highest catalytic performance for the reduction and decolorization of 4-NA and Congo red (CR). Additionally, the enhanced catalytic performance was observed for the reduction of 2-NP, 3-NP, and 4-NP as well. Arumugam *et al.*[84] used *N*-2′,3′-dihydroxy propyl 1,4-diazobicyclo[2.2.2] octanium chloride, *N*-2′,3′-dihydroxy propyl-1-methyl-2-pyrrolidonium chloride, and *N*-2′,3′-dihydroxy propyl-2-amino pyridinium chloride (ionic liquids) as an organic component, while boron nitride nanosheets were used as an inorganic component for the effective development of CuFe$_2$O$_4$. The catalytic performance of the TCPIL/CuFe$_2$O$_4$/BNONS nanomaterial was investigated using 2-NA, 3-NA, 4-NA, 4-nitro-2-phenylenediamine (4-NPDA), as well as MB as model contaminants. Kundu *et al.*[58] showed the synthesis of Ag NPs immobilized on silica spheres. They deposited gelatin-stabilized silver nanoparticles onto a silica matrix, and found excellent catalytic performance for the reduction of 4-NA. Kong *et al.*[45] reported

the usage of polyaniline/iron oxide NP nanocomposites as a capping agent, and examined the assembly of gold and palladium nanoparticles inside the polyaniline/iron oxide NP nanocomposite. They also studied the catalytic efficiency through the reduction of 4-NA. Liu *et al.*[85] reported the synthesis of pGO-NM hybrids using GO as an inorganic material with poly(amidoamine) PAMAM 3.0 G dendrites as an organic matrix to evaluate the catalytic efficiency of 4-NA. The results revealed that the polarity of GO in the PAMAM-modified GO (rGO) was enhanced due to the presence of the amino group of the dendrimer on the surface of GO. Organic–inorganic supporting assemblies for the catalytic reduction of 4-NA are summarized in Table 4.

Characterization

Characterization techniques involved in the study of the engineered nanocatalysts are presented in Table 5.

Fundamentals of the catalytic reduction of 4-NA

Kinetics

The technique of UV-visible spectroscopy is usually utilized for carrying out the mechanistic, as well as kinetic, studies of this particular reaction. In terms of kinetics, a literature survey showed that a 4-NA reduction reaction generally followed pseudo first-order kinetics. By monitoring the concentration of

Table 4 Inorganic–organic hybrid assemblies for the catalytic degradation of 4-NA

| Nanocatalytic assembly | | | | | | Catalytic reduction of 4-NA | | | |
Nanomaterial	Inorganic fabrication medium	Organic fabrication medium	Diameter (nm)	Pollutant	Recyclability	Reductant	Solvent	Reaction settings	Ref.
Fe$_3$O$_4$ NMs	Reduced graphene oxide	Poly(amidoamine)	—	4-NA	—	—	Aqueous solution	[Catalyst] = 10 mg, [4-NA] = 5.8 × 10^{-3} M L^{-1}	85
Au	Fe$_3$O$_4$	Polydopamine	12–45	2-NA, 3-NA, 4-NA, 2-NT, 3-NT, 4-NT, 2-NCB, 2,4-DNT	8th > 98%	NaBH$_4$	Aqueous solution	[Catalyst] = 1 × 10^{-5} M, [4-NA] = 1 × 10^{-3} M, [NaBH$_4$] = 5 × 10^{-3} M	86
CuFe$_2$O$_4$	Boron nitride nanosheets	N-2',3'-Dihydroxy propyl-1,4-diazobicyclo[2.2.2]octanium chloride, N-2',3'-dihydroxy propyl-1-methyl-2-pyrrolidonium chloride, N-2',3'-dihydroxy propyl-2-amino pyridinium chloride (ionic liquids)	20	MB, AR, 4N2PDA, 3NA, 4NA, 2NA	—	NaBH$_4$	Aqueous solution	[Catalyst] = 0.2 mg mL^{-1}, [4-NA] = 0.01 M, [NaBH$_4$] = 0.5 M	84
Au	Graphene oxide	Polyamidoamine (PAMAM) dendrimer	—	4-NP, 4-NA, 2-NA, 3-NA, NB, and other nitroaromatics	—	NaBH$_4$	Aqueous solution	[Catalyst] = 5 mg, [4-NA] = 0.01 M, [NaBH$_4$] = 0.1 M	87
Cu	Fe$_3$O$_4$ nano particle	Citric acid	25–35	NB, 4-NP, 4-NA and other nitroarenes	8	NaBH$_4$	Aqueous solution	[Catalyst] = 20 mg, [4-NA] = 1 × 10^{-3} M, [NaBH$_4$] = 5 × 10^{-3} M	88
Cu	1,6-Diaminohexane (DAH)	Polystyrene-*block*-polyacrylic acid (PS-b-PAA)	3	4-NA, 4-NP	18	NaBH$_4$	Aqueous solution	[Catalyst] = 20 mg, [4-NA] = 1 × 10^{-3} mol L^{-1}, [NaBH$_4$] = 2 × 10^{-3} M	89
Ag	Silica	Gelatin	16 ± 4 nm	4-NA, 4-NP	—	NaBH$_4$	Aqueous solution	[Catalyst] = 5.3 × 10^{-3} g, [4-NA] = 4.3 × 10^{-4} M, [NaBH$_4$] = 1 × 10^{-1} M	58
Au, Pd	Fe$_3$O$_4$	Polyaniline	—	4-NA	—	NaBH$_4$	Aqueous solution	[Catalyst] = 0.2 mL, [4-NA] = 4 × 10^{-4} M, [NaBH$_4$] = 30 × 10^{-3} M	45

Table 5 Properties of different catalytic systems utilized for 4-NA reduction

Catalytic system	Analytical techniques	Remarks	Ref.
Au NPs	XRD, TEM, HR-TEM, SEM, UV-VIS, FTIR	Soapnut shell-mediated gold nanoparticles showed efficient catalytic activity. Gold nanoparticles chemically reduced 4-nitroaniline into 4-PDA. The UV-visible spectroscopy results suggested that 1 mM of $HAuCl_4$ possessed better catalytic properties.	50
	FTIR, XRD, TEM, SEM, UV-VIS	Formation of gold nanoparticles was confirmed by XRD. TEM displayed various shapes of Au NPs formed with varying concentrations of IPE. UV-Vis spectra showed the reduction of 4-NA.	48
	XRD, FTIR, UV-VIS, DLS, EDX, TEM, HR-TEM	SEM and EDS confirmed that the gold nanoparticles possessed a crystalline nature and size in the nano-range. UV-Vis spectra displayed the reduction of 4-NA into 4-PDA.	49
	XRD, FTIR, UV-VIS, DLS, EDX	Reduction of 4-NA using Au NPs was observed by UV-visible spectroscopy. The TEM image showed that the Au NPs were spherical in shape, having an average size of 16 nm.	51
Ag NPs	XRD, FTIR, UV-VIS, DLS, EDX	Reduction of 4-NA using Au NPs, Ag NPs were observed by UV-visible spectroscopy. The TEM image showed that the Au NPs and Ag NPs were spherical in shape, having average sizes of 16 nm and 20 nm.	51
	TEM, SEM, UV-VIS, FTIR	Ag NPs were self-assembled into a two-dimensional sub-monolayer structure on a glass slide surface confirmed by SEM. Raman spectra showed that in the absence of a catalyst, the reduction proceeded very slowly. However, 4-NA reduction was completed within 27 min in the presence of a catalyst.	36
	XRD, TEM, SEM, UV-VIS, FTIR	Cefditorene-mediated Ag NPs were small-sized and monodispersed, as confirmed by TEM. UV-Visible spectroscopy examined changes in the absorbance. At 240 nm, a new peak appeared within 2 min, confirming the 4-PDA formation.	42
	XRD, TEM, UV-VIS, DLS	TEM analysis showed that the Ag nanospheres had a hollow spherical structure. DLS showed a hydrodynamic diameter within the range of 10–40 nm, and UV visible spectra showed the reduction of 4-NA.	38
$Fe_3O_4/SiO_2/Ag$	TEM, HR-TEM, SQUID, EDS, XRD, UV-VIS	The XRD pattern confirmed the face-centered cubic structure of Ag in $Fe_3O_4/SiO_2/Ag$. UV-Vis spectra showed that reduction was completed within 200 s.	31
Flower-like Bi_2S_3 microspheres	XRD, TEM, HR-TEM, SEM, UV-VIS, EDS	Metash 6100 UV-Vis spectrophotometer monitored the reducing reaction of 4-NA into 4-PDA.	44
Au nano crystals	SEM, UV-VIS, TEM, XPS	TEM analysis showed that the size of the rhombic dodecahedron was 71.8 nm. UV-Vis analysis confirmed that the rhombic dodecahedral gold nanocrystals showed the best catalytic activity, as compared to the octahedral and cubic gold nanocrystals.	90
Ag NWS-rGO	FTIR, XRD, TEM, FE-SEM, UV-VIS	GO reduction was confirmed by XDR and UV-VIS analysis. UV-Vis absorption spectra confirmed the reduction of 4-NA.	52
BPS-30 capped gold nanoparticles	XRD, TEM, UV-VIS	UV-Vis absorption spectroscopy examined the yield of the gold nanoparticles and evaluated the reduction of 4-NA.	55
Ag-p(NiPA-co-AAc) hybrid microgels	FTIR, XRD, TEM, SEM, UV-VIS, DLS	XRD indicated the crystalline nature of the Ag NPs. DLS analysis showed that the hydrodynamic diameter of the microgel particles increased significantly in the pH range of 4–7. At pH $\geq$ 8, no change in the hydrodynamic diameter was observed with an increase in the temperature due to the dominant pH effect.	6
PVP- Au NPs	FTIR, XPS, TEM, HR-TEM, EDS, SEM, UV-VIS, XRD	Spherical shape of the Au NPs confirmed by TEM analysis. XPS technique resolved the chemical identity of the atoms through the measured binding energy.	57
Au–Pd bimetallic nanoparticles	TEM, EDS, SEM, UV-VIS	SEM analysis showed the average size of 7–10 nm for the Au–Pd bimetallic nanoparticles grown on porous germania. UV-Vis analysis showed the complete reduction of 4-NA in 4 min, with a rate constant of 53×10^{-2} min^{-1} in the presence of bimetallic Au–Pd nanoparticles.	13
FeAgPt trimetallic NPs	FTIR, XPS, TEM, EDS, SEM, UV-VIS, XRD, EDAX	Crystalline nature of the FeAgPt trimetallic NPs confirmed by XRD and EDX analysis. TEM, UV-VIS and FTIR studies	91

Table 5 (Contd.)

Catalytic system	Analytical techniques	Remarks	Ref.
		confirmed that *Platycodon grandiflorum* root extract acted as an excellent stabilizing and reducing agent for the FeAgPt trimetallic NPs.	
TCPIL/CuFe$_2$O$_4$/ BNONS nanomaterial	FTIR, XPS, UV-VIS, XRD, EDS, SEM, DSC-TGA, TEM, HR-TEM, STEM, AFM	The successful formation of bimetallic CuFe$_2$O$_4$ NPs, their stability, identification, functional group analysis and composition or morphologies were confirmed by XRD, EDS, SEM, DSC-TGA, TEM, HR-TEM, STEM, AFM and FTIR techniques. UV-Vis spectra showed that the catalyst effectively improved (complete reduction in 30 min) the photocatalytic performance of 4-NA.	84

4-NA measured at a particular time 't', the apparent rate constant (k_{app}) for the reaction can be measured as indicated by eqn (1). Since the reaction is considered pseudo first-order, the concentration of sodium borohydride is taken in excess. The reaction was only found to be dependent on the concentration of 4-NA. Eqn (1), representing the pseudo first-order kinetics, is represented as follows:

$$\ln[C_t/C_o] = -k_{aap}t \tag{1}$$

where C_t is the concentration of 4-NA at any reaction time 't', while C_o is the concentration of 4-NA at the start of the reaction. The ratio of concentrations can also be written in terms of absorbance since absorbance is directly related to concentration. Hence, the above equation, in terms of absorbance, is as follows:

$$\ln[A_t/A_o] = -k_{aap}t \tag{2}$$

where A_t is the absorbance of 4-NA at any reaction time 't', while A_o is the absorbance of 4-NA at the start of the reaction. This equation shows the applicability of UV-Vis spectroscopy as a monitoring tool for the 4-NA reduction because the measured absorbance directly relates to the concentration of the dye

present in the medium. Edison et al.[82] found that the 4-NA reduction in the presence of Ag NPs as a catalyst and NaBH$_4$ as a reducing agent followed pseudo first-order reaction kinetics. A linear relationship between $\ln(A_t/A_o)$ and the time for the reduction of 4-NA was observed. The rate constant of 4-NA in aqueous medium was found to be 11.16×10^{-3} s^{-1}. Farooqi et al.[6] reported a reduction of 4-NA using Ag-p(NiPA-co-AAc) hybrid microgels as the catalyst and NaBH$_4$ as the reductant. They observed that the reaction followed pseudo-first order kinetics owing to the presence of an excess concentration of the reductant. The catalytic rate equation for 4-NA can be given as:

$$-d[4NA]/dt \propto [NaBH_4][4NA] \tag{3}$$

$$-d[4NA]/dt = k'[NaBH_4][4NA] \tag{4}$$

$$-d[4NA]/dt = k_{aap}[4NA] \tag{5}$$

$$-d[4NA]_t/[4NA]_o = k_{aap}t \tag{6}$$

$$\ln[A_t/A_o] = -k_{aap}t \tag{7}$$

Here, A_t is the concentration of 4-NA at time t (min) and A_o is the initial concentration of 4-NA. Kundu et al.[39] observed that the

Table 6 Values of rate constant, order of reaction and reaction time obtained in the reduction of 4-NA utilizing different catalytic systems

Catalyst used	Order of reaction	Rate constant (min^{-1})	Reaction completion time (min)	Ref.
Au NPs	Pseudo first-order kinetics	9.1×10^{-5}	Not available	51
Ag NPs		7.67×10^{-5}		
Au NPs	First-order kinetics	4.5×10^{-2}	59	50
Au NPs	Pseudo first-order kinetics	6.5×10^{-2}	6	48
Ag NPs	Not available	Not available	2	42
Colloidal hollow silver nanoparticles	Pseudo first-order kinetics	4.2×10^{-2}	10	38
BPS-30 capped gold nanoparticles	First-order kinetics	1.52×10^{-1}	25	55
Ag-P(NIPAM-AAc-AAm) hybrid microgels	Pseudo first-order kinetics	6.06×10^{-1}	22	59
Gold nano crystals	First-order kinetics	1.8717×10^{-1}	12.5	90
Ag NWS-rGO	Pseudo first-order kinetics	1.7034×10^{-4}	4	52
Pt NPs/GA	First-order kinetics	4.4×10^{-1}	10	46
Ag-p(NiPA-co-AAc) hybrid microgels	Pseudo first-order kinetics	9.41×10^{-2}	Not available	6
CuNPs-chiston	Pseudo first-order kinetics	7.51×10^{-3} s^{-1}	6	69

conversion of 4-NA into 4-PDA followed first-order kinetics using gold nanoparticles as a catalyst. The rate constant was found to be 2.083×10^{-2} min^{-1} and the first order rate equations are given below:

$$\ln[C] = 0.0208t + \ln[C_o] \tag{8}$$

$$\ln[C_t/C_o] = -k_{aap}t \tag{9}$$

It was also observed that the reduction of 4-NA through Au NPs showed the fastest catalytic activity as compared to other metal nanoparticles. Zhang et al.[46] reported that the reduction of 4-NA by the Pt NPs/graphene aerogel (GA) catalyst also followed first-order kinetics with a rate constant of 0.44 min^{-1} (Table 6). Farooqi et al.[6] reported that Ag NPs work as an efficient catalyst for the reduction of 4-NA. Ag NPs act as an electron relay center, transferring electrons from BH_4^{-1} to 4-NA. These reactions were monitored in the absence and presence of a catalyst. It was found that in the absence of the catalyst, the system cannot overcome the kinetic barrier present between the reductant and dye molecules. Begum et al.[59] also designed pH- and temperature-sensitive silver nanoparticles fabricated in poly(N-isopropylacrylamide-acrylic acid-acrylamide) Ag-P(NIPAM-AAc-AAm) hybrid microgel catalysts for the conversion of 4-NA into 4-PDA using NaBH$_4$ as a reducing agent. Farooqi et al.[64] synthesized silver nanoparticles fabricated in poly(N-isopropylacrylamide-co-allyl acetic acid) Ag-p(NIPAM-co-AAAc) hybrid microgels, and observed that there was no change in the absorbance $[\ln(A_t/A_o)]$ with time. This indicated that the 4-NA reduction had not been initialized. This duration represents an induction period during which the diffusion or adsorption of reactants on the surface of the nanoparticles occurs. After the induction period, a decrease in the absorbance was observed with time, which indicated that the reaction was progressing and the reduction of 4-NA had been started.

Thermodynamics

Along with kinetic studies, the thermodynamic parameters are also important for the catalytic degradation of 4-NA. The thermodynamic parameters can be acquired by utilizing the pre-acquired information from the kinetics studies. Drawing the plot between the apparent rate constant (k_{app}) and the temperature variations is utilized to find out the activation energy (E_a). The intercept of the acquired plot presents the value of the Arrhenius pre-exponential parameter. Eqn (10) represents the following parameters:

$$\ln k_{app} = -\frac{E_a}{R}\frac{1}{T} + \ln A \tag{10}$$

Here, R represents the general gas constant, E_a is the activation energy and A is the Arrhenius pre-exponential parameter. From our literature survey, it was determined that the kinetic studies, including the value of k_{aap} and the order of the reaction, have been widely documented as compared to the thermodynamic studies. Amongst all articles cited in this manuscript, few articles documented any information regarding the thermodynamic activation energy parameter for the degradation of 4-

NA.[92] In addition, other thermodynamic parameters (e.g., entropy of activation ($\Delta S^\#$) and enthalpy of activation ($\Delta H^\#$)) can also be attained by placing the Boltzmann constant (k_B) and Plank's constant (h) values in the Eyring equation below:

$$\ln\left(\frac{k_{app}}{T}\right) = \ln\left(\frac{k_B}{h}\right) + \frac{\Delta S^\#}{R} - \frac{\Delta H^\#}{R}\frac{1}{T} \tag{11}$$

Maity et al.[66] studied the thermodynamic parameters (i.e., enthalpy of activation and entropy change) using a hydrogel system, but no information has been documented for these parameters for the reduction of 4-NA. In addition, eqn (10) and (11) have not been widely reported for the catalytic degradation of 4-NA. Hence, more consideration should be given towards a better understanding of the 4-NA degradation in the future.

Mechanism for reduction of 4-NA

A plausible mechanism for the reduction of nitroaromatic compounds in the presence of NPs and NaBH$_4$ is widely reported in the academic literature. The reactants including the 4-NA molecules and reducing agents are added in the reaction mixture. They immediately diffuse inside and become adsorbed on the attachment site on the surface of the nanoparticle. This adsorption is reversible and occurs very rapidly. NPs act as an electron transfer medium between the adsorbed molecules. The catalyst enhances the transmission of an electron from a donor-reducing agent (BH_4^{-1}) to acceptor dye molecules (4-NA).[93] This electron transfer occurs from the catalyst surface to 4-NA to reduce the nitro group into the amino group.[39] Moreover, NPs form a NP–H complex through their interaction with the hydrogen gas released from the reductant (NaBH$_4$). A hydrogen bond is formed by the reaction between the oxygen and hydrogen atoms of 4-NA and the NPs–H complex, respectively. Hence, these complexes not only assist in capturing the 4-NA from aqueous media but also enhance the reduction rate. Moreover, on the surface of the nanocatalysts, the instantaneous adsorption of the hydrogen species or diffusion of the adsorbed species occurs, which leads to desorption of the product.[82] Abbas et al.[31] successfully demonstrated the reduction of 4-NA using the Fe$_3$O$_4$/SiO$_2$/Ag nanocube, Ag NPs, and SiO$_2$/Ag. They reported that the Fe$_3$O$_4$/SiO$_2$/Ag nanocube proved to be an efficient catalyst as compared to Ag NPs and SiO$_2$/Ag due to the presence of ferrous ion in the iron oxide structure, which improves the hydroxyl ion production rate. Liu et al.[37] showed that NaBH$_4$ alone (in the absence of a catalyst) could not reduce 4-NA because of the kinetic barrier, which restricted the transfer of an electron from donor BH_4^{-1} to acceptor 4-NA. Hence, the catalyst Ag NPs/PSi chip effectively improved the degradation efficiency of 4-NA. Kundu et al.[39] successfully prepared cetyltrimethylammonium bromide-terminated gold (Au) nanomaterials, including nanospheres, nanorods, and nanoprisms. It was observed that the Au nanospheres proved to be an efficient catalyst, as compared to the nanorods and nanoprisms, owing to its smaller surface area as shown in Fig. 5.

Gnanaprakasam and Selvaraju[52] investigated the catalytic activity of Ag NPs/nanowires decorated on reduced graphene oxide (rGO) sheets through the reduction of 4-NA. They showed that rGO alone did not show any catalytic activity, but Ag nanowires immobilized on rGO exhibited the best catalytic activity towards the reduction of 4-NA. They also reported clear absorption spectra of 4-NA due to a small amount of the nanocatalyst. Zhang et al.[46] studied the reduction of 4-NA by using the heterogeneous catalyst of platinum (Pt) NPs loaded on a graphene aerogel (GA) [Pt NPs/GA]. Pt NPs/GA could effectively reduce 4-NA within a very short time (10 min), which was confirmed by the absorption spectrum, i.e., decreasing peak intensity at 381 nm.

Reuse of catalyst

The catalyst could be reprocessed in many ways, e.g., repeated washing of the catalyst or by centrifugation. Guo et al.[44] reported that the used catalyst could work efficiently four times for the catalytic reduction of 4-NA. The catalytic efficiency decreased after the first cycle, but 67% catalytic efficiency could be attained within 9 min. Moreover, after the first cycle, the shape of the catalyst degraded and the specific surface area was decreased. In addition, the active sites were reduced and the catalytic efficiency was decreased. Fig. 6 showed the catalytic reusability of various nanocatalytic assemblies. Abbas et al.[31] reported that the $Fe_3O_4/SiO_2/Ag$ nanocubes showed an 88% catalytic efficiency for the reduction of 4-NA with
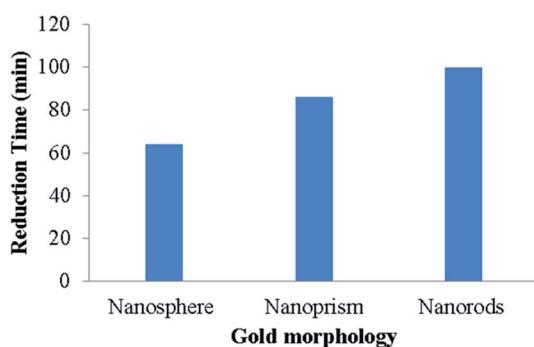
Fig. 5 Effect of nanomaterial shape on the reduction of 4-NA.[39]
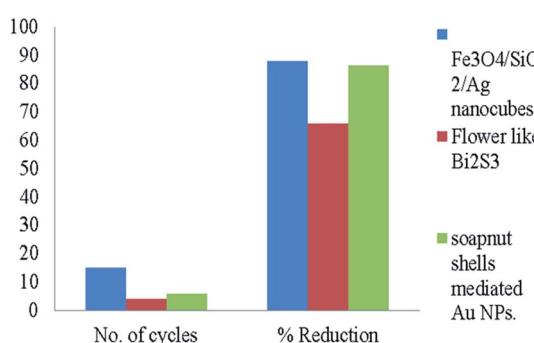
Fig. 6 Comparison based on the recyclability of various catalysts used for 4-NA reduction.[31,44,50]

recycling properties of up to 15 cycles. Reddy et al.[50] showed that soapnut shell-mediated gold nanoparticles are a potent recyclable nanocatalyst, having an 86.4% catalytic efficiency for up to 6 recycling reduction cycles. Bakhsh et al.[69] also evaluated the catalytic stability of the Cu NPs-chitosan catalyst supported on filter paper. They found that the catalyst could work efficiently for up to four consecutive cycles for the successful reduction of 4-NA. Moreover, Tables 1–3 showed the recyclability of various nanocatalytic assemblies supported on various capping agents.

Summary and future goals

To conclude, an extensive survey on the recent improvements regarding the enhancement of the chemical reduction capabilities of various catalytic systems containing different metallic NPs has been presented in this study. The presence of a reductant is not sufficient for carrying out the reduction of 4-NA, owing to the presence of the kinetic barrier. The presence of the nanocatalytic surface allows the reaction to proceed by providing the required electron-transferring surface between the reactants involved. The reduction of 4-NA is of critical need due to its hazardous nature and non-biodegradability. It is evident that supporting materials improve the catalytic capabilities of nanocatalysts by keeping the nanomaterial in the nanodomain via effective immobilization. Consequently, the generation of a less toxic and industrially useful product (4-PDA) from the reduction of 4-NA by various nanocatalysts is a highly researched methodology for dealing with this particular dye. The organic systems include the biological systems, although they are utilized for the immobilization of the nanomaterials. However, the system itself is biodegradable and cannot withstand extreme working conditions. Inorganic assemblies resolve the issue of the effective immobilization owing to their rigid nature, but they still need improvement in terms of their biodegradability issues. Hybrid assemblies containing both the organic and inorganic components seem to be the main recent advancement in terms of the supporting medium, as it combines the properties of both the organic and inorganic systems in one single system. The literature survey confirms that 4-NA reduction follows pseudo first-order kinetics. However, much work still needs to be done to study its thermodynamic parameters. The main advantage in making these nanocatalysts and their reduction economical is that the utilized catalyst can be detached from the reaction medium easily and reused several times without a significant loss in its efficiency.

Although the recent advancements introduced in the field of nanocatalysis are quite significant and advanced, work is still required in certain aspects of this field. As reported in this review, most of the articles used $NaBH_4$ as a reductant for the catalytic degradation of 4-NA, which is highly toxic in nature. The use of green reductants (hydrogen gas and other naturally present reductants) should be encouraged in the future for 4-NA reduction. It is evident from the literature survey that Au NPs, along with Ag NPs, are preferably utilized for 4-NA reduction. However, these NPs are very expensive. Cheap metal

nanoparticles (such as Cu, Ni, Fe, Co) must be fabricated and stabilized for the degradation of 4-NA. A greener approach that is non-toxic, cheap and eco-friendly in nature should be used frequently for the synthesis and stabilization of the metal nanoparticle catalysts. Immobilization supports must be developed from waste materials instead of expensive membranes to make the catalytic reduction more economical. Instead of using the green extract in its crude form, the compounds responsible for carrying out the stabilization and reduction must be identified, isolated and utilized in the immobilization of NPs so that the drawbacks of leakage and ineffective immobilization can be removed in the case of the green chemistry approach. Moreover, thermodynamic parameters (*i.e.*, entropy and energy of activation) using the Arrhenius and Eyring formulas should be applied for 4-NA reduction. Additionally, catalyst recycling along with TOF must be studied using 4-NA as a model contaminant.

Abbreviations

4-NA	4-Nitroaniline
2-NA	2-Nitroaniline
3-NA	3-Nitroaniline
2-NT	2-Nitrotoluene
3-NT	3-Nitrotoluene
4-NT	4-Nitrotoluene
4-NP	4-Nitrophenol
2,4-DNT	2,4-Dinitrotoluene
2-NCB	2-Nitrochloro-benzene
4-PDA	4-Phenylenediamine
$NaBH_4$	Sodium borohydride
KBH_4	Potassium borohydride
Fe_3O_4	Iron oxide
NW	Nanowires
TMRA	Tetra methyl resorcinol arene tetra amino amide
BS-Au NPs	Bare surface gold nanoparticles
Bi_2S_3	Bismuth sulfide
Au NPs	Gold nanoparticles
Ag NPs	Silver nanoparticles
GO	Graphene oxide
rGO	Reduced graphene oxide
GH	Graphene hydrogel
GA	Graphene aerogel
L-Cs	L-Cysteine
SM	Silica matrix
p-ANE	Polyaniline
SiO_2	Silica
pVpy	Poly vinyl pyridine
FESEM	Field emission scanning electron microscopy
TEM	Transmission electron microscopy
XRD	X-ray diffraction
TOF	Turnover frequency

Conflicts of interest

There are no conflicts to declare.

References

1 Z. H. Farooqi, R. Khalid, R. Begum, U. Farooq, Q. Wu, W. Wu, M. Ajmal, A. Irfan and K. Naseem, *Environ. Technol.*, 2018, 1–10, DOI: 10.1080/09593330.2018.1435737.

2 S. Silambarasan and A. S. Vangnai, *J. Hazard. Mater.*, 2016, **302**, 426–436.

3 R. Begum, R. Rehan, Z. H. Farooqi, Z. Butt and S. Ashraf, *J. Nanopart. Res.*, 2016, **18**, 231.

4 Y. S. Zhao, C. Sun, J. Q. Sun and R. Zhou, *Sep. Purif. Technol.*, 2015, **142**, 182–188.

5 F. Bhunia, N. C. Saha and A. Kaviraj, *Ecotoxicology*, 2003, **12**, 397–404.

6 Z. H. Farooqi, A. Ijaz, R. Begum, K. Naseem, M. Usman, M. Ajmal and U. Saeed, *Polym. Compos.*, 2018, **39**, 645–653.

7 K. Li, Z. Zheng, J. Feng, J. Zhang, X. Luo, G. Zhao and X. Huang, *J. Hazard. Mater.*, 2009, **166**, 1180–1185.

8 A. Qureshi, V. Verma, A. Kapley and H. J. Purohit, *Int. Biodeterior. Biodegrad.*, 2007, **60**, 215–218.

9 K. Li, Y. Li and Z. Zheng, *J. Hazard. Mater.*, 2010, **178**, 553–559.

10 M. I. Din, J. Najeeb, Z. Hussain, R. Khalid and G. Ahmad, *Inorg. Nano-Met. Chem.*, 2020, 1–7.

11 M. I. Din, M. Tariq, Z. Hussain and R. Khalid, *Inorg. Nano-Met. Chem.*, 2020, 1–6.

12 D. S. Lee, K. S. Park, Y. W. Nam, Y.-C. Kim and C. H. Lee, *J. Hazard. Mater.*, 1997, **56**, 247–256.

13 M. R. Regan and I. A. Banerjee, *Scr. Mater.*, 2006, **54**, 909–914.

14 K. Li, Z. Zheng, J. Feng, J. Zhang, X. Luo, G. Zhao and X. Huang, *J. Hazard. Mater.*, 2009, **166**, 1180–1185.

15 W. Ma and Y. Fang, *J. Colloid Interface Sci.*, 2006, **303**, 1–8.

16 T. Tanaka, A. Nakajima, A. Watanabe, T. Ohno and Y. Ozaki, *J. Mol. Struct.*, 2003, **661**, 437–449.

17 J. Liu, Y. Li and K. Li, *J. Environ. Chem. Eng.*, 2013, **1**, 389–397.

18 R. Holze, *Electrochim. Acta*, 1990, **35**, 1037–1044.

19 K. Zheng, B. Pan, Q. Zhang, W. Zhang, B. Pan, Y. Han, Q. Zhang, D. Wei, Z. Xu and Q. Zhang, *Sep. Purif. Technol.*, 2007, **57**, 250–256.

20 P. L. T. X. L. Huafei and Z. Xiaojun, *Environ. Prot. Chem. Ind.*, 2008, **1**.

21 S. Peixoto, E. Silva, C. Costa, R. Nery, F. Rodrigues, J. Silva, R. Bezerra and R. Soares, *Aquacult. Nutr.*, 2018, **24**, 579–585.

22 A. Saupe, *Chemosphere*, 1999, **39**, 2325–2346.

23 M. I. Din, R. Khalid and Z. Hussain, *Anal. Lett.*, 2018, **51**, 892–907.

24 S. Gautam, S. P. Kamble, S. B. Sawant and V. G. Pangarkar, *Chem. Eng. J.*, 2005, **110**, 129–137.

25 Y. Wang, Y.-n. Zhang, G. Zhao, M. Wu, M. Li, D. Li, Y. Zhang and Y. Zhang, *Sep. Purif. Technol.*, 2013, **104**, 229–237.

26 J.-H. Sun, S.-P. Sun, M.-H. Fan, H.-Q. Guo, Y.-F. Lee and R.-X. Sun, *J. Hazard. Mater.*, 2008, **153**, 187–193.

27 J.-H. Sun, S.-P. Sun, M.-H. Fan, H.-Q. Guo, L.-P. Qiao and R.-X. Sun, *J. Hazard. Mater.*, 2007, **148**, 172–177.

28 M. I. Din, R. Khalid and Z. Hussain, *Sep. Purif. Rev.*, 2020, 1–18, DOI: 10.1080/15422119.2020.1714658.

29 R. V. Jagadeesh, G. Wienhöfer, F. A. Westerhaus, A.-E. Surkus, M.-M. Pohl, H. Junge, K. Junge and M. Beller, *Chem. Commun.*, 2011, **47**, 10972–10974.

30 X. Bai, Y. Gao, H.-g. Liu and L. Zheng, *J. Phys. Chem. C*, 2009, **113**, 17730–17736.

31 M. Abbas, S. R. Torati and C. Kim, *Nanoscale*, 2015, **7**, 12192–12204.

32 H.-S. Lee and Y.-W. Lin, *Ann. Occup. Hyg.*, 2009, **53**, 289–296.

33 K. Mohammed, A. Chowdhury and M. Rasul, *Energies*, 2015, **8**, 7522–7541.

34 G. Zhan, P. Li and H. C. Zeng, *Adv. Mater.*, 2018, **30**, 1802094.

35 M. I. Din, R. Khalid, Z. Hussain, T. Hussain, A. Mujahid, J. Najeeb and F. Izhar, *Crit. Rev. Anal. Chem.*, 2019, 1–17.

36 Q. Zhou, G. Qian, Y. Li, G. Zhao, Y. Chao and J. Zheng, *Thin Solid Films*, 2008, **516**, 953–956.

37 X. Liu, H. Cheng and P. Cui, *Appl. Surf. Sci.*, 2014, **292**, 695–701.

38 R. Vadakkekara, M. Chakraborty and P. A. Parikh, *Colloids Surf.*, 2012, **399**, 11–17.

39 S. Kundu, S. Lau and H. Liang, *J. Phys. Chem. C*, 2009, **113**, 5150–5156.

40 N. Toshima and T. Yonezawa, *New J. Chem.*, 1998, **22**, 1179–1201.

41 A. B. Madavi, S. U. Nandanwar and M. Chakraborty, *Part. Sci. Technol.*, 2016, 1–10.

42 Y. Junejo, E. Karaoğlu and A. Baykal, *J. Inorg. Organomet. Polym. Mater.*, 2013, **23**, 970–975.

43 J. Grigas, E. Talik and V. Lazauskas, *Phys. Status Solidi B*, 2002, **232**, 220–230.

44 F. Guo, Y. Ni, Y. Ma, N. Xiang and C. Liu, *New J. Chem.*, 2014, **38**, 5324–5330.

45 L. Kong, X. Lu, E. Jin, S. Jiang, X. Bian, W. Zhang and C. Wang, *J. Solid State Chem.*, 2009, **182**, 2081–2087.

46 X. Zhang, D. Liu, L. Yang, L. Zhou and T. You, *J. Mater. Chem. A*, 2015, **3**, 10031–10037.

47 M. Tumma and R. Srivastava, *Catal. Commun.*, 2013, **37**, 64–68.

48 C. Shi, N. Zhu, Y. Cao and P. Wu, *Nanoscale Res. Lett.*, 2015, **10**, 1–8.

49 K. Anand, R. Gengan, A. Phulukdaree and A. Chuturgoon, *J. Ind. Eng. Chem.*, 2015, **21**, 1105–1111.

50 V. Reddy, R. S. Torati, S. Oh and C. Kim, *Ind. Eng. Chem. Res.*, 2012, **52**, 556–564.

51 P. Dauthal and M. Mukhopadhyay, *Korean J. Chem. Eng.*, 2015, **32**, 837–844.

52 P. Gnanaprakasam and T. Selvaraju, *RSC Adv.*, 2014, **4**, 24518–24525.

53 C. Shi, N. Zhu, Y. Cao and P. Wu, *Nanoscale Res. Lett.*, 2015, **10**, 147.

54 S. Francis, S. Joseph, E. P. Koshy and B. Mathew, *Artif. Cells, Nanomed., Biotechnol.*, 2018, **46**, 795–804.

55 H. Jia, X. Gao, Z. Chen, G. Liu, X. Zhang, H. Yan, H. Zhou and L. Zheng, *CrystEngComm*, 2012, **14**, 7600–7606.

56 A. Leelavathi, T. U. B. Rao and T. Pradeep, *Nanoscale Res. Lett.*, 2011, **6**, 123.

57 S. Kundu, K. Wang and H. Liang, *J. Phys. Chem. C*, 2009, **113**, 5157–5163.

58 S. Kundu, M. Mandal, S. K. Ghosh and T. Pal, *J. Colloid Interface Sci.*, 2004, **272**, 134–144.

59 R. Begum, K. Naseem, E. Ahmed, A. Sharif and Z. H. Farooqi, *Colloids Surf.*, 2016, **511**, 17–26.

60 Y. Yao, Y. Sun, Y. Han and C. Yan, *Chin. J. Chem.*, 2010, **28**, 705–712.

61 J. Najeeb, G. Ahmad, S. Nazir, K. Naseem and A. Kanwal, *Korean J. Chem. Eng.*, 2017, 1–16.

62 M. I. Din, R. Khalid, F. Akbar, G. Ahmad, J. Najeeb and Z. U. Nisa Hussain, *Soft Mater.*, 2018, **16**, 228–247.

63 Z. H. Farooqi, N. Tariq, R. Begum, S. R. Khan, Z. Iqbal and A. Khan, *Turk. J. Chem.*, 2015, **39**, 576–588.

64 Z. H. Farooqi, R. Begum, K. Naseem, U. Rubab, M. Usman, A. Khan and A. Ijaz, *Russ. J. Phys. Chem. A*, 2016, **90**, 2600–2608.

65 Z. H. Farooqi, K. Naseem, A. Ijaz and R. Begum, *J. Polym. Eng.*, 2016, **36**, 87–96.

66 I. Maity, D. B. Rasale and A. K. Das, *Soft Matter*, 2012, **8**, 5301–5308.

67 T. Vincent, F. Peirano and E. Guibal, *J. Appl. Polym. Sci.*, 2004, **94**, 1634–1642.

68 Y. Liang, C. Lin, J. Guan and Y. Li, *RSC Adv.*, 2017, **7**, 7460–7468.

69 E. M. Bakhsh, F. Ali, S. B. Khan, H. M. Marwani, E. Y. Danish and A. M. Asiri, *Int. J. Biol. Macromol.*, 2019, **131**, 666–675.

70 Y. Choi, H. S. Bae, E. Seo, S. Jang, K. H. Park and B.-S. Kim, *J. Mater. Chem.*, 2011, **21**, 15431–15436.

71 K. Jasuja, J. Linn, S. Melton and V. Berry, *J. Phys. Chem. Lett.*, 2010, **1**, 1853–1860.

72 M. M. Raju and D. K. Pattanayak, *RSC Adv.*, 2015, **5**, 59541–59549.

73 U. Nithiyanantham, S. R. Ede and S. Kundu, *J. Mater. Chem. C*, 2014, **2**, 3782–3794.

74 P. S. Rathore, R. Patidar, T. Shripathi and S. Thakore, *Catal. Sci. Technol.*, 2015, **5**, 286–295.

75 Z. Liu, J. Du, X. Jin, P. Li, X. Jiang and J. Yuan, *Mater. Lett.*, 2019, **237**, 9–13.

76 K. Mishra, T. N. Poudel, N. Basavegowda and Y. R. Lee, *J. Catal.*, 2016, **344**, 273–285.

77 S. K. Ghosh, M. Mandal, S. Kundu, S. Nath and T. Pal, *Appl. Catal., A*, 2004, **268**, 61–66.

78 P. Deka, R. Choudhury, R. C. Deka and P. Bharali, *RSC Adv.*, 2016, **6**, 71517–71528.

79 Y. Yao, M. Xue, Z. Zhang, M. Zhang, Y. Wang and F. Huang, *Chem. Sci.*, 2013, **4**, 3667–3672.

80 Y. Zhang, F. Gao and M.-L. Fu, *Chem. Phys. Lett.*, 2018, **691**, 61–67.

81 T. N. J. I. Edison, M. G. Sethuraman and Y. R. Lee, *Res. Chem. Intermed.*, 2016, **42**, 713–724.

82 T. N. J. I. Edison, E. R. Baral, Y. R. Lee and S. H. Kim, *J. Cluster Sci.*, 2016, **27**, 285–298.

83 F. Ali, S. B. Khan, T. Kamal, K. A. Alamry, E. M. Bakhsh, A. M. Asiri and T. R. Sobahi, *Carbohydr. Polym.*, 2018, **192**, 217–230.

84 V. Arumugam, P. Sriram, T.-J. Yen, G. G. Redhi and R. M. Gengan, *Appl. Catal., B*, 2018, **222**, 99–114.

85 X. Liu, T. Zhao, H. Cheng, C. Zhu, S. Li and P. Cui, *Appl. Surf. Sci.*, 2015, **327**, 226–232.

86 T. Zeng, H.-y. Niu, Y.-r. Ma, W.-h. Li and Y.-q. Cai, *Appl. Catal., B*, 2013, **134**, 26–33.

87 R. Rajesh and R. Venkatesan, *J. Mol. Catal. A: Chem.*, 2012, **359**, 88–96.

88 P. Viswanathan, T. Bhuvaneswari and R. Ramaraj, *Colloids Surf.*, 2017, **528**, 48–56.

89 Q. Diao, X. Li, M. Diao, Y.-I. Lee and H.-G. Liu, *J. Colloid Interface Sci.*, 2018, **522**, 272–282.

90 C.-Y. Chiu, P.-J. Chung, K.-U. Lao, C.-W. Liao and M. H. Huang, *J. Phys. Chem. C*, 2012, **116**, 23757–23763.

91 N. Basavegowda, K. Mishra and Y. R. Lee, *J. Alloys Compd.*, 2017, **701**, 456–464.

92 M. Shahid, Z. H. Farooqi, R. Begum, K. Naseem, M. Ajmal and A. Irfan, *Korean J. Chem. Eng.*, 2018, 1–9.

93 A. Hernández-Gordillo and V. R. González, *Chem. Eng. J.*, 2015, **261**, 53–59.